Journal of Solid State Chemistry 183 (2010) 2051–2058

Contents lists available at ScienceDirect

Journal of Solid State Chemistry

journal homepage: www.elsevier.com/locate/jssc

Bixbyite- and anatase-type phases in the system Sc–Ta–O–N

A. Stork [a], H. Schilling [a], C. Wessel [b], H. Wolff [b], A. Börger [c], C. Baehtz [d], K.-D. Becker [c], R. Dronskowski [b], M. Lerch [a,*]

[a] Institut für Chemie, TU Berlin, Straße des 17. Juni 135, D-10623 Berlin, Germany
[b] Institut für Anorganische Chemie, RWTH Aachen, Landoltweg 1, D-52056 Aachen, Germany
[c] Institut für Physikalische und Theoretische Chemie, TU Braunschweig, Hans-Sommer-Str. 10, D-38106 Braunschweig, Germany
[d] HASYLAB at DESY, Netkestr. 85, D-22603 Hamburg, Germany

ARTICLE INFO

Article history:
Received 21 May 2010
Received in revised form
5 July 2010
Accepted 7 July 2010
Available online 15 July 2010

Keywords:
Tantalum
Scandium
Oxide nitrides
Ammonolysis
Bixbyite
Anatase
Baddeleyite

ABSTRACT

The aim of our study was to modify the basis compound ß-TaON, which crystallizes in the monoclinic baddeleyite-type, by incorporation of appropriate dopant ions, in order to obtain anion-deficient cubic fluorite-type phases, which are of interest as solids with mobile nitrogen ions. For this purpose, scandium-doped tantalum oxide nitrides were prepared by ammonolysis of amorphous oxide precursors. An unexpected variety of phases with different structural features was observed: bixbyite-type phases of general composition $Sc_xTa_{1-x}(O,N)_y$ with $0.33 \le x \le 1$ and $1.7 \le y \le 1.9$, yellow colored metastable anatase-type phases such as $Sc_{0.1}Ta_{0.9}O_{1.2}N_{0.8}$ or $Sc_{0.15}Ta_{0.85}O_{1.3}N_{0.7}$ and, additionally, anosovite-type phases $Sc_xTa_{3-x}O_{2x}N_{5-2x}$ with $0 \le x \le 1.05$. Selected phases were investigated by UV/vis spectroscopy. Anatase- and anosovite-type compounds show brilliant colors. In the anatase-type phase, a possible anion ordering was examined by theoretical methods. Additionally, energy calculations on phase stability were performed for $Sc_xTa_{1-x}O_{1+2x}N_{1-2x}$ in the baddeleyite, rutile, and anatase structure types with varying amounts of dopants.

© 2010 Elsevier Inc. All rights reserved.

1. Introduction

Transition metal oxide nitrides are an interesting group of materials with physical properties making them candidates for technical applications. For example, they are in the focus of recent studies testing their suitability as photocatalysts for water splitting under sunlight [1–3]. Ionic conductivity studies focusing on the behavior of N^{3-} anions have yielded promising results, indicating the possibility of N^{3-} ion conducting materials [4–6]. On the other hand, the substitution of cadmium sulfoselenide pigments by non-toxic tantalum oxide nitrides would have great environmental benefits [7,8]. Transition metal oxide nitrides are also candidates suitable for dielectrics in microelectronic devices [9,10] or as chemical gas sensors [11]. In this contribution, we focus on possible nitrogen ion conductivity and optical properties of Sc-doped tantalum oxide nitride and nitride phases.

The materials presented in this study are derived from the basic components TaON and Ta_3N_5. The well-known ß-TaON [12] crystallizes in the monoclinic baddeleyite-type structure. It can be considered as nitrogen-rich analogue of monoclinic zirconia and is prepared most easily by treatment of Ta_2O_5 at ~900 °C for 16 h with flowing water-saturated ammonia gas [13]. Recent theoretical calculations of the electronic structure of ß-TaON gave a band gap of 2.4 eV [14]. Its olive color as it is obtained by ammonolysis is not in accord with the typical light absorption behavior of semiconductor pigments. This is probably due to a small content of reducible metal oxides in the Ta_2O_5 starting material. After a short reoxidation treatment in air, ß-TaON becomes yellow [15]. Pauling's 2nd rule predicts an ordered distribution of O and N on the two anion sites, which is confirmed by neutron diffraction experiments [16]. ZrO_2-like phase transitions from the monoclinic baddeleyite-type to tetragonal or cubic fluorite-type phases, at higher temperatures, have not been detected yet. This may be explained by the relatively low decomposition temperature (~1100 °C) of TaON. However, a high pressure phase transition at ~31 GPa to the cotunnite-type structure with ninefold coordinated cations has been predicted by theoretical methods [17]. The stability and electronic structure of several polymorphs (baddeleyite, anatase, rutile and fluorite) of TaON have recently been studied by theoretical methods, including features like anion ordering [18]. A reported hexagonal α-TaON modification [19] had already been shown to be inconsistent with quantum-chemical calculations [20] and it is unlikely that alpha-TaON is actually a stable phase. A new metastable polymorph (γ-TaON) exhibiting the VO_2(B)-type structure has been described recently [21]. Ta_3N_5 [22,23] crystallizes in the anosovite-type (Ti_3O_5) structure. It can be obtained as brick-red powder by ammonolysis of Ta_2O_5 with dry ammonia at 900 °C. Ta_3N_5 has a UV/vis absorption edge at ~600 nm corresponding to a band gap of 2.1 eV. Absolute

* Corresponding author. Fax: +49 30 314 79656.
E-mail address: lerch@chem.tu-berlin.de (M. Lerch).

0022-4596/$ - see front matter © 2010 Elsevier Inc. All rights reserved.
doi:10.1016/j.jssc.2010.07.006

energies of the valence and conduction band determined by UPS and electrochemical measurements are in excellent agreement with such a band gap [24].

Thinking about fast nitrogen ion conduction, anion-deficient fluorite-type phases, as known from quaternary zirconium oxide nitrides, are of interest [5]. Whereas zirconium-based materials are limited by a poor N/O ratio within their stability fields, ß-TaON derived phases, partially doped with lower-valent cations, are candidates for nitrogen-rich anion-deficient phases of the fluorite-type. Keep in mind that the above-mentioned high-temperature polymorphs of zirconia can be stabilized to an ambient temperature by doping with aliovalent oxides, such as yttria or scandia. The resulting zirconia phases with randomly distributed oxygen vacancies show outstanding oxygen mobility at high temperatures and are commonly used in fuel cells or sensors. First investigations of Mg-doped TaON result in the formation of anatase phases [25]. Brilliant in color, the anatase-type compounds are not of interest as fast anion conductors because they exhibit no significant amount of anion vacancies. Interestingly, partial substitution of tantalum by yttrium leads to the formation of anion-deficient quaternary fluorite-type oxide nitrides [26]. Unfortunately, quantum-chemical calculations on the mobility of nitrogen ions in tantalum-based oxide nitrides yielded an activation energy of ~2.4 eV for the Y-doped phases [27]. It should be emphasized that Sc-doped phases appear most promising candidates because of their low activation energy for the nitrogen ion jump process of ~1.7 eV, which is lower than that observed in zirconium oxide nitride based materials with significant nitrogen ion mobility (~2.0 eV [28]). As a consequence, in our study, we focus on the possibilities of substituting TaON partially with scandium. In addition, both Sc-doped TaON and Ta_3N_5-phases are of interest as pigments with possibly brilliant colors in the range between yellow and red.

2. Experimental

2.1. Synthesis

Amorphous ternary phases in the system Sc–Ta–O were prepared, using a modified Pecchini method [29]. Tantalum chloride (Alfa Aesar, 99.99%) was dissolved in ethanol containing citric acid in an excess of 12 times the $TaCl_5$. Any dispersed Ta_2O_5 can be removed by centrifugation. The resulting tantalum citrate complexes are insensitive to water. A stock solution with a defined content of tantalum citrate has been prepared. Scandium chloride (99.9%, anhydrous, Sigma-Aldrich) was dissolved in ethanol which contains citric acid in an excess of 12 times the $ScCl_3$. Appropriate quantities of the two citrate solutions were mixed together and ethylene glycol in an excess of 17 times the metals content was added. The solvent and HCl were evaporated and the citrate complexes together with ethylene glycol have been polymerized at ~150 °C. The organic residues of the polymer were burnt off at 600 °C for 16 h to give white X-ray amorphous powders. A series of mixed oxides $Sc_xTa_{1-x}O_{2.5-x}$ with x=0.025, 0.05, 0.075, 0.10, 0.15, 0.20, 0.25, 0.30, 0.33, 0.35, 0.40, 0.45, 0.50, 0.60, 0.70, 0.80, and 0.90 was prepared this way. The amorphous mixed oxides were converted into oxide nitrides by ammonolysis with either dry (3.8, Air Liquide) or water-saturated ammonia gas at constant flow rates between 5 and 50 l/h at temperatures of 700, 800 or 900 °C for 16 h.

2.2. Characterization

Nitrogen and oxygen contents were determined using a LECO TC-300/EF-300 N/O analyzer (hot gas extraction). Ta_2O_5 and Si_3N_4 were used as standard materials for calibration. The accuracy is ~2% of the true N/O. The Sc content was checked by an EDX using a Hitach S2700. A Siemens D5000 powder diffractometer (Cu-$K\alpha_1$ radiation, λ=154.06 pm, position sensitive detector, Ge monochromator) was used for XRD measurements at an ambient temperature. Temperature dependent measurements (samples in SiO_2-glass capillaries under argon) were carried out with a STOE STADI-P powder diffractometer (Mo-$K_{\alpha1}$ radiation, λ=70.93 pm, imaging plate detector) equipped with a graphite heated resistance furnace. Synchrotron X-ray diffraction measurements were performed at the Hamburger Synchrotronstrahlungslabor (HASYLAB, beamline B2, λ=70.99 pm). The program POWDER CELL 2.4 [30] was used for preliminary quantitative phase analysis and lattice parameter determination, FULLPROF 2000 [31] for Rietveld refinements. Peak profiles were fitted with a pseudo-Voigt function.

UV/vis spectra were recorded with a Perkin-Elmer Lambda 900 spectrometer equipped with a Harrick "Praying Mantis" accessory for diffuse reflection, using KCl as reference. Absorbance-related spectra were calculated from the measured diffuse reflectances using the Kubelka–Munk formula:

$$F(R) = \frac{(1-R)^2}{2R} = \varepsilon c \frac{1}{s}$$

where R is the reflectance, ε is the absorption coefficient, c the concentration of absorbing species, and s the scattering coefficient.

Band-gaps E_g were calculated using the modified Tauc equation ($h\nu \geq E_g$)

$$[F(R)h\nu]^{\frac{1}{\beta}} = h\nu - E_g$$

where $h\nu$ is the photon energy, β a coefficient depending on the nature of the optical transition (1/2 for an allowed direct transition, 2 for an allowed indirect transition).

2.3. Computational details

The electronic-structure calculations were performed using the Vienna *ab initio* simulation package (VASP) [32,33], which is based on density-functional theory (DFT) and uses fast pseudopotential basis sets (plane waves). Projected augmented waves (PAW) [34] were used and contributions of correlation and exchange were treated in the generalized-gradient approximation (GGA) as described by Perdew, Burke and Ernzerhof [35]. An energy-cutoff of 500 eV and a sampling of 21 irreducible k-points ensured well-converged structures. During the optimization process, the atomic positions and the lattice parameters were allowed to relax until the ionic convergence criterium of 10^{-5} eV was reached.

3. Results and discussion

In order to prepare Sc-doped tantalum oxide nitride and nitride phases, amorphous mixed oxides $Sc_xTa_{1-x}O_{2,5-x}$ with x=0.05, 0.10, 0.15, 0.20, 0.25, 0.30, 0.33, 0.35, 0.40, 0.45, 0.50, 0.60, 0.70, 0.80, and 0.90 were treated with dry ammonia for 16 h at 700 °C. Generally, single-phase samples of bixbyite-type structure are obtained for Sc contents above ~35 cation% (Fig. 1). As the bixbyite-type can be described as an anion-deficient fluorite-type, these phases are of interest as anion conductors. In contrast, for scandium contents below 20 cation% single-phase samples with the Ta_3N_5-structure are synthesized at 900 °C. The use of water-saturated ammonia gas for nitridation and a slightly higher temperature of 800 °C led to the formation of anatase-type phases. These Ta_3N_5- or anatase-derived compounds are promising candidates for color pigments.

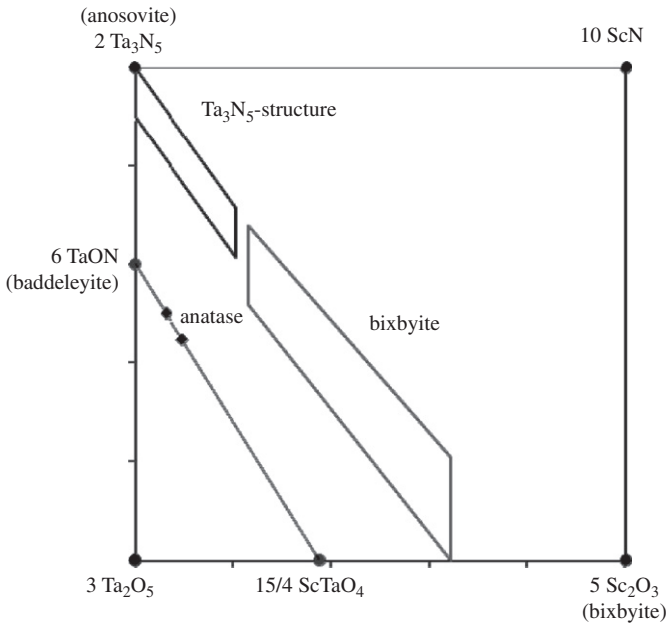

Fig. 1. Schematic representation of all new compounds obtained as single-phase samples in the system Sc–Ta–O–N (dark grey symbols).

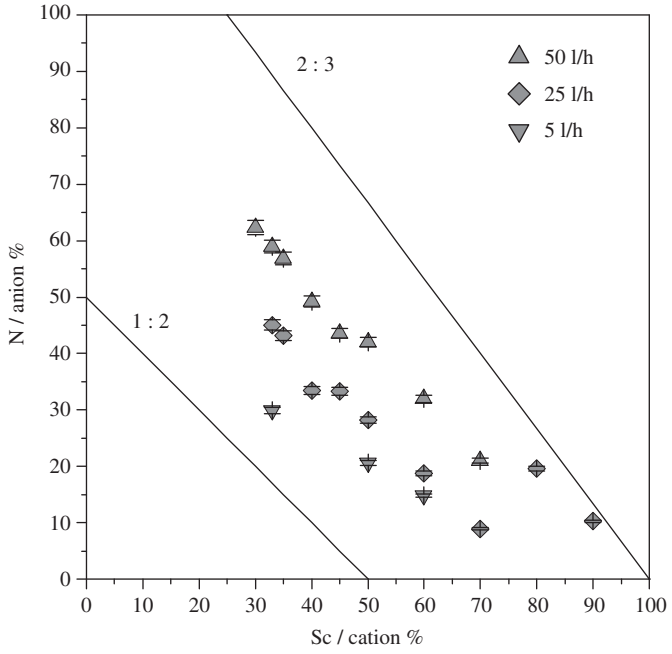

Fig. 2. Chemical compositions of the three sets of ammonolysis products obtained with dry ammonia at 700 °C at different gas flow rates. Lines: cation to anion ratios 1:2 (ideal fluorite-type stoichiometry) and 2:3 (ideal bixbyite-type stoichiometry).

3.1. Bixbyite-type phases in the system Sc–Ta–O–N

For variation of the anion vacancy concentration, important to optimize the anion mobility, three series of single-phase bixbyite-type products were synthesized, one at an ammonia flow rate of 5 l/h, one at 25 l/h and another at 50 l/h. Generally, with increasing flow rate, the nitrogen contents of the resulting phases increase. Chemical compositions of all specimen within these three series of materials are depicted in Fig. 2. The cation:anion ratios range between 1:2 (fluorite-type structure without anion vacancies) and 2:3 (bixbyite-type structure, fluorite-type derived with long-range ordered anion vacancies, 25% anion vacancies for an ideal 2:3 stoichiometry).

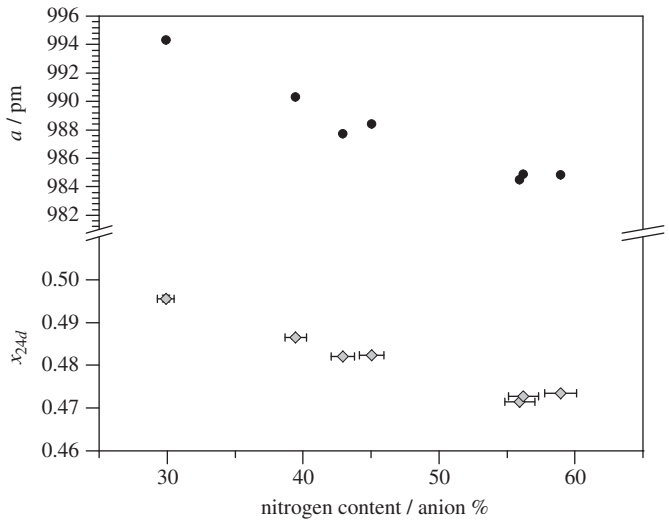

Fig. 3. Lattice parameters a and cationic x parameters for bixbyite-type phases with 33 cation% Sc as a function of the nitrogen content.

Compared to fluorite-type phases in the system Y–Ta–O–N [26], bixbyite-type phases in the system Sc–Ta–O–N exhibit much higher nitrogen concentrations. They show a wide variation of the nitrogen content at the same Sc concentration, depending on the conditions of ammonolysis. With increasing ammonia flow rates during synthesis, phases of higher nitrogen and lower oxygen content are formed. For detailed investigation of the effect of nitrogen content on the structural parameters, a set of oxide nitrides with 33 cation% Sc and varying nitrogen concentrations was prepared at ammonia flow rates between 5 and 50 l/h. Fig. 3 shows the lattice parameters as a function of the determined nitrogen concentration. A decrease of a from 994.30(3) pm at 29.9 anion% N to 984.82(2) pm at 59.0 anion-% N was observed. The reason for this effect is the relaxation of the lattice around the vacancies. Cubic bixbyite-type phases crystallize in space group $Ia\bar{3}$; (Sc/Ta)1 is located on an 8a site (0,0,0), (Sc/Ta)2 on a 24d (x,0,1/4) site, and the anions on a 48e (x,y,z) site. It should be mentioned that there are no indications for cation ordering from our refinements. Consequently, the site occupation factors were fixed for the final refinements. Due to the X-ray methods used in this study, the superlattice reflections observed for bixbyite in comparison to the fluorite-type are mainly caused by the deviation of the x parameter of the 24d site from the value of $\frac{1}{2}$ which is fixed for the cubic fluorite structure. In parallel with the decrease of the lattice parameter, the deviation of the 24d x parameter from the ideal value of $\frac{1}{2}$ increases, leading to significant superlattice reflections in the X-ray powder diagram. Comparing the X-ray powder patterns of phases with low and high vacancy concentrations, it is evident that for low concentrations the patterns are very similar to those of fluorite-type phases (Fig. 4). It should be mentioned that long-range ordered arrangements of O and N are a disadvantage for high anion mobility. As known from bixbyite-type Zr_2ON_2, determination of the N/O distribution for this particular type of crystal structure is problematic even if a combination of X-ray and neutron diffraction methods is used [36,37]. Quantum-chemical methods provide a trustworthy model of the ground state [38], clearly preferring a random distribution of the anions.

The structural chemistry of bixbyite-type phases in the system Sc–Ta–O–N is similar to that of the non-stoichiometric uranium nitrides. Here, compositions from U_2N_3 (bixbyite-type) [39] to

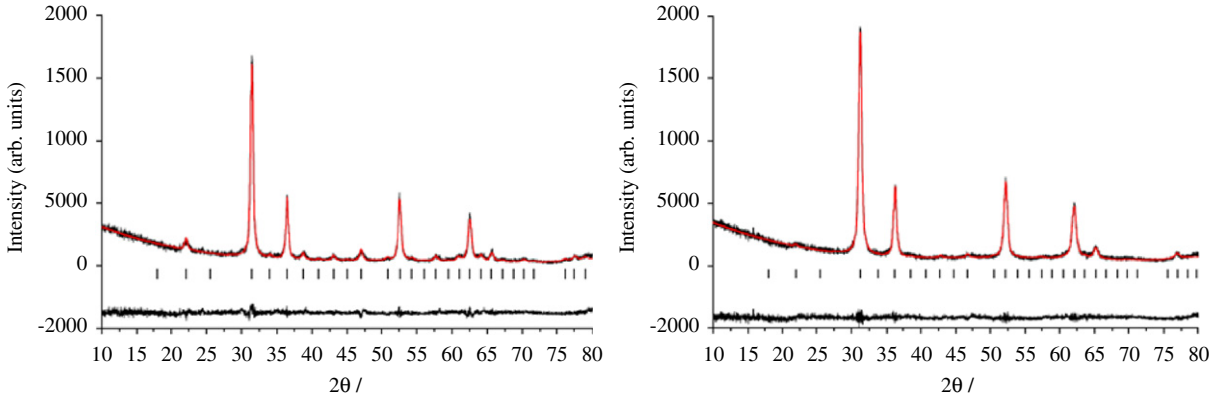

Fig. 4. X-ray powder diagram of $Sc_{0.33}Ta_{0.67}O_{0.69}N_{0.99}$ (left) and $Sc_{0.33}Ta_{0.67}O_{1.10}N_{0.72}$ (right) with results of the Rietveld refinement.

Table 1
Optical absorption characteristics of Sc-doped phases with Ta_3N_5-structure.

Composition	Abs. edge (nm)	Band-gap* (eV)	Unit cell volume (pm^3)
Ta_3N_5	600	2.06	408.65×10^6
$Sc_{0.3}Ta_{2.7}O_{0.6}N_{4.4}$	570	2.18	409.68×10^6
$Sc_{0.6}Ta_{2.4}O_{1.2}N_{3.8}$	550	2.25	410.56×10^6
$Sc_{0.9}Ta_{2.1}O_{1.8}N_{3.2}$	475	2.61	412.16×10^6

* Diffuse reflectance powder spectra, Fig. 5, evaluated for direct allowed transitions. For indirect transitions, band-gaps turn out smaller than this by 0.2–0.4 eV.

UN_2 (fluorite-type) [40] can be realized. It should be mentioned that a wide range of composition is also reported for bixbyite-type Zr_2ON_2 (γ-phase) [36], extending from $\sim Zr_2O_{0.7}N_{2.2}$ ($AX_{1.45}$) to $\sim Zr_2O_{1.6}N_{1.6}$ ($AX_{1.6}$). γ-Zr_2ON_2 undergoes a phase transition into a cubic fluorite-type phase at $\sim$800 °C with partial decomposition to ZrN. Sc–Ta–O–N bixbyite-type phases are expected to show the same phase transformation at lower temperatures, as their compositions ($\sim AX_{1.68}$ to $\sim AX_{1.88}$) are closer to AX_2. This is of importance for high-temperature anion conductivity because randomly distributed vacancies are a prerequisite for high anion mobility in fluorite-type derived phases. Interestingly, high-temperature X-ray diffraction experiments did not show any order–disorder transition up to 900 °C for our phases. Evidently, the bixbyite structure with its ordered arrangement of anion vacancies is stable up to such high temperatures. Consequently, bixbyite-type Sc–Ta–O–N phases are not useful as fast anion conductors.

3.2. Nitrogen-rich anosovite-type phases in the system Sc–Ta–O–N

As mentioned above, Ta_3N_5-type phases are observed for small amounts of scandium. These phases were prepared by ammonolysis of amorphous mixed oxides $Sc_xTa_{1-x}O_{2.5-x}$ with $0 \le x \le 0.35$ in dry ammonia at 900 °C. Single-phase samples can be obtained containing up to $\sim$35 cation% Sc. For larger contents also bixbyite-phases are found. The suggested general composition $Sc_xTa_{3-x}O_{2x}N_{5-2x}$ is supported by N/O-analysis (see also [25]). Therefore, there is no significant amount of anion vacancies. As expected, due to the larger ionic radius of Sc^{3+} compared to Ta^{5+}, the unit cell volume of Sc-doped Ta_3N_5-phases increases with increasing Sc content (Table 1). UV/vis spectra of powder samples with Sc concentrations of 10, 20 or 30 cation% Sc were recorded, Fig. 5. With increasing Sc and O content, the absorption edge (Table 1) shifts towards shorter wavelengths, in agreement with

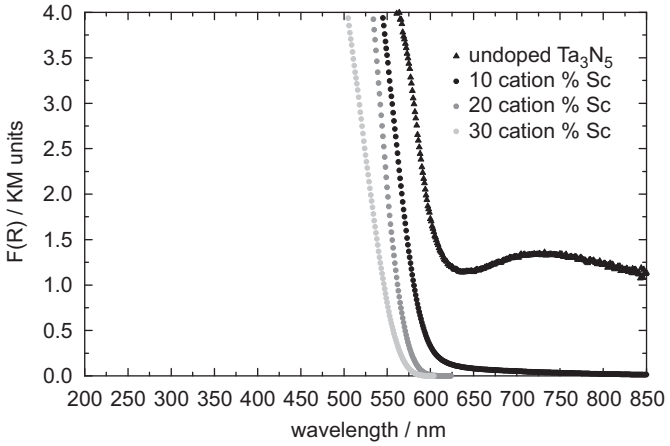

Fig. 5. UV/vis powder spectra of pure Ta_3N_5 and Ta_3N_5-phases with Sc contents of 10, 20 and 30 cation%, respectively.

the concept of Phillips [41], van Vechten [42], and Jorgensen [43]. The maximum shift was observed for 30 cation% Sc. The steepness of the absorption edges is a reason for the brilliant colors of the powder samples. The steepness gives also evidence of good crystallinity of the samples and of a high degree of homogenization of the mixed coordination polyhedra of anions and cations in the $Sc_xTa_{3-x}O_{2x}N_{5-2x}$ solid solutions. As already mentioned, the local structure in the anosovite-type solid solutions is not disturbed by structural anion or cation vacancies. In this context, it may be worth pointing out that systems containing high concentrations of disordered structural vacancies, see for example $Y_6WO_{12-3x}N_{2x}\square_{2+x}$ solid solutions, where $\square$ denotes a structural anion vacancy, do not possess absorption edges with steepnesses suitable for application as pigments [44].

3.3. Anatase-type phases in the system Sc–Ta–O–N

As known from the Mg–Ta–O–N system [25], anatase-type oxide nitrides show brilliant yellow–orange colors. Consequently, we also prepared compounds of that structure type in the Sc-containing system. The observed crystalline phases after ammonolysis (800 °C) of the amorphous mixed oxides $Sc_xTa_{1-x}O_{2.5-x}$ with $0 \le x \le 0.5$ are depicted in Fig. 6. Single-phase anatase-type samples of yellow color were obtained at Sc contents of $x = 0.1$ and 0.15. For lower Sc concentrations, the amount of anatase-type phase decreases, while the baddeleyite-phase is dominant. Additionally,

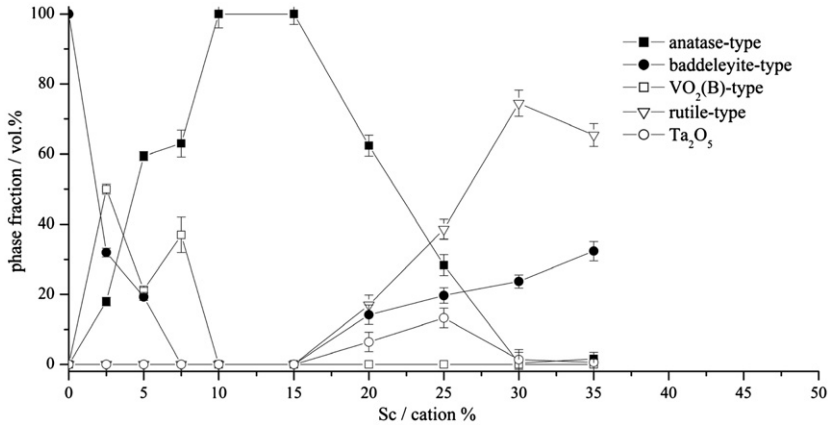

Fig. 6. Observed phases (determined by quantitative XRD-analysis) in the system Sc–Ta–O–N obtained by ammonolysis with water-saturated ammonia at 800 °C.

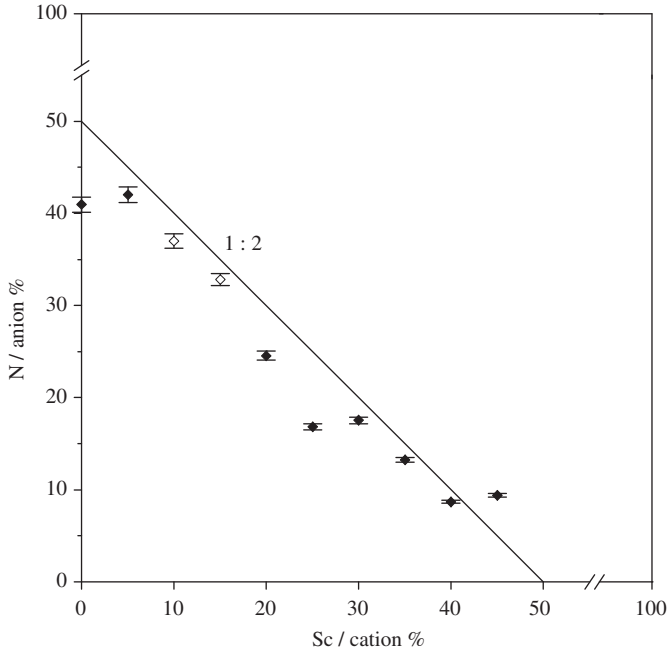

Fig. 7. Chemical compositions of the ammonolysis products obtained with water-saturated ammonia gas at 800 °C. Hollow symbols: single-phase products. Line: cation to anion ratio 1:2.

γ-TaON-type phases are obtained with a maximum phase fraction of ~50% for $x=0.025$. In contrast, for $x=0.3$, the sample consists mainly of a rutile-type phase (~80%). Quantitative determinations of the phase contents for $x \geq 0.4$ were not possible due to the poor crystallinity of the products. The chemical compositions of the samples are represented graphically (Fig. 7) as lying roughly on a straight line between TaON (0 cation% Sc; 50 anion% N) and $ScTaO_4$ (50 cation% Sc; 0 anion% N) (Fig. 1), which corresponds to a 1:2 stoichiometry indicating no significant amount of anion vacancies. The general composition on this line is $Sc_xTa_{1-x}O_{1+2x}N_{1-2x}$. The compositions of the anatase-type single phases are therefore given as $Sc_{0.1}Ta_{0.9}O_{1.2}N_{0.8}$ and $Sc_{0.15}Ta_{0.85}O_{1.3}N_{0.7}$. From a formal point of view, the compounds can be described as solid solutions of TaON and $ScTaO_4$:

$$Sc_{0.1}Ta_{0.9}O_{1.2}N_{0.8} = 0.8\ TaON \cdot 0.1\ ScTaO_4$$

$$Sc_{0.15}Ta_{0.85}O_{1.3}N_{0.7} = 0.7\ TaON \cdot 0.15\ ScTaO_4$$

As mentioned above, the absence of vacancies and a highly ordered crystal structure have to be considered as important prerequisite for brilliant colors of the powders. $Sc_{0.15}Ta_{0.85}O_{1.3}N_{0.7}$ was chosen for detailed structural investigations. It was indexed in respect to space group $I4_1/amd$ with lattice parameters a=392.472(2) pm and c=1014.11(2) pm (Tables 2 and 3). The c/a ratio is 2.58. From synchrotron X-ray diffraction data (Fig. 8), no deviation from the tetragonal metric was detected. There are also no indications for cation ordering. In order to analyze a possible ordering of the oxide and nitride anions, calculations using density-functional theory were performed. In space group $I4_1/amd$, suggested by X-ray diffraction experiments (see Table 3), only one anionic site exists. In contrast, three of the *translationsgleich* subgroups possess two independent anionic sites for the anatase structure: $I\bar{4}m2$, $I4_1/md$, and *Imma*, and these are depicted in Fig. 9. In all those subgroups, the cations are octahedrally coordinated, but the octahedra differ in their arrangements of the oxide and nitride anions, as shown in Fig. 10. In the structures with *Imma* and $I4_1/md$ symmetry, the coordination polyhedron around the tantalum cation

Table 2
Refined structural data for $Sc_{0.15}Ta_{0.85}O_{1.3}N_{0.7}$.

Structure type	Anatase
Formula weight	190.86 g/mol
Space group	$I4_1/amd$
Crystal system	Tetragonal
Lattice parameters	a=392.472(2) pm c=1014.11(2) pm c/a=2.58
Unit cell volume	$V=156.20\times10^6$ pm3
Formula units	$Z=4$
Calculated density	$\rho=8.15$ g/cm^3
Diffractometer	B2/HASYLAB
Wavelength	70.990 pm
Number of profile points	11,249
2θ Range	5–50°
Number of refined parameters	32
R_{wp}	5.1%
R_{Bragg}	7.6%
R_{exp}	1.7%
S	3.0

Table 3
Refined atomic parameters for anatase-type $Sc_{0.15}Ta_{0.85}O_{1.3}N_{0.7}$ (space group $I4_1/amd$).

Atom	*Wyck.*	*x*	*y*	*z*	Occ.	B_{iso}/Å^2
Ta/Sc	4b	0	1/4	3/8	0.85/0.15	0.27(3)
N/O	8e	0	1/4	0.5886(7)	0.35/0.65	1.1(2)

consists of TaO_3N_3, while in $I\bar{4}m2$ two different octahedra with the compositions TaO_4N_2 and TaO_2N_4 are present. This causes a destabilization of the structure as indicated in Table 4. The most stable ordering scheme is the structure with space group $I4_1/md$, favored by 5 kJ/mol compared with $I\bar{4}m2$ and by 3 kJ/mol compared to *Imma* symmetry. In order to examine whether an ordered structure is favored at all, a calculation without any appreciable anionic ordering was performed. Table 4 implies that such a disordered structure is 13 kJ/mol less stable than the ordered structure with space group $I4_1/md$. Thus, the theoretical calculations indicate an anionic ordering in $Sc_{0.15}Ta_{0.85}O_{1.3}N_{0.7}$ with symmetry $I4_1/md$. The structural parameters for anatase-type $Sc_{0.15}Ta_{0.85}O_{1.3}N_{0.7}$ in space group $I4_1/md$ are listed in Table 5.

In order to understand the effect of scandium doping on the stabilities of possible structure types, energy calculations of $Sc_xTa_{1-x}O_{1+2x}N_{1-2x}$ in the baddeleyite, rutile and anatase types with varying dopant amounts ($x=0.00$, 0.05, 0.10, 0.15) were performed. In Fig. 11, the energy difference of the structure types is depicted as a function of the scandium content. For undoped TaON, baddeleyite is the most stable polymorph, in good correspondence with experimental findings [45]. However, already for small amounts of dopant, the baddeleyite structure is destabilized. According to theoretical calculations, the anatase – and, furthermore, the rutile type – should be preferred in comparison to the baddeleyite-type in Sc–**Ta–O**–N for $x \geq 0.05$. For a dopant level of $x=0.10$ and $x=0.15$, the anatase structure results as a single-phase product, while for $x=0.05$, the phase composition consists of 60% anatase-type (see Fig. 6). The order of stability of the three polymorphs corresponds to the theoretical findings for Mg–**Ta–O**–N [46], where the baddeleyite-type is also destabilized upon doping with magnesium.

Thinking about an application as high-temperature color pigments, thermal stability and expansion are of importance. As shown by DTA/TG measurements in air, $Sc_{0.15}Ta_{0.85}O_{1.3}N_{0.7}$ reacts with oxygen to give the colorless oxide at temperatures above 450 °C. In argon atmosphere, a phase transformation from the metastable anatase phase to the baddeleyite-type structure is observed in the temperature region between 950 and 1050 °C (Fig. 12). The

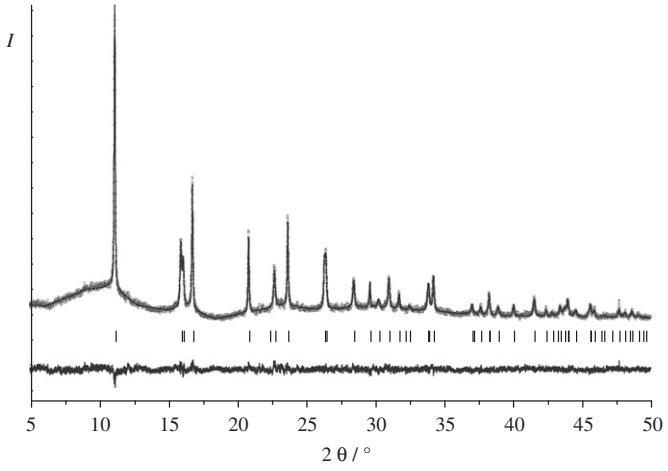

Fig. 8. X-ray powder diffraction diagram (synchrotron) of anatase-type $Sc_{0.15}Ta_{0.85}O_{1.3}N_{0.7}$ with results of the Rietveld refinement.

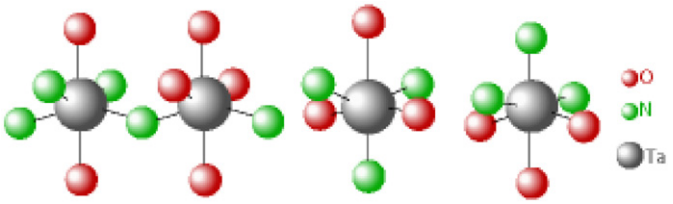

Fig. 10. Octahedral coordination of tantalum in the structures with the symmetries $I\bar{4}m2$ (left), $I4_1/md$ (middle) and *Imma* (right).

Table 4
Results of the calculations in terms of anionic ordering.

Space group	Energy per f.u. (eV)	ΔE per f.u. (kJ/mol)
$I\bar{4}m2$	−29.853	5
$I4_1/md$	−29.904	0
Imma	−29.877	3
Disordered	−29.769	13

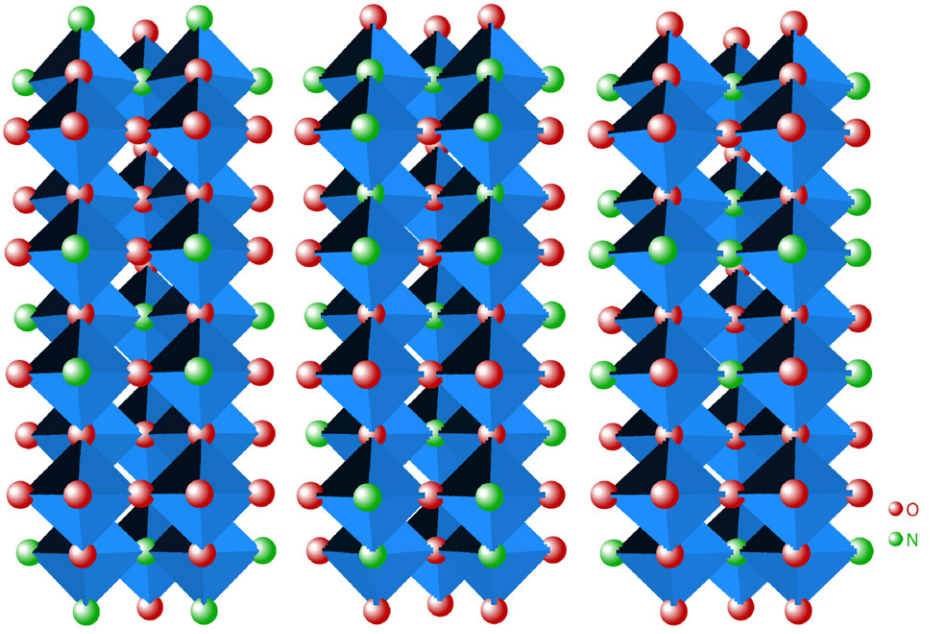

Fig. 9. The three *translationsgleich* subgroups with two independent anionic sites in $Sc_{0.15}Ta_{0.85}O_{1.3}N_{0.7}$: $I\bar{4}m2$ (left), $I4_1/md$ (middle) and *Imma* (right).

Table 5
Structural parameters for anatase-type $Sc_{0.15}Ta_{0.85}O_{1.3}N_{0.7}$ in space group $I4_1/md$ as deduced from X-ray diffraction experiments and density-functional theoretical calculations.

		Atom	*Wyck.*	*x*	*y*	*z*	Occ.
X-ray							
$a=b$	3.925 Å	Ta/Sc	4*a*	0	0	0	0.85/0.15
c	10.141 Å	O/N	4*a*	0	0	0.214	0.65/0.35
Z	4	O/N	4*a*	0	$\frac{1}{2}$	0.036	0.65/0.35
V	156.20 Å^3						
DFT-GGA							
a	3.944 Å	Ta/Sc	4*a*	0	0	0	0.85/0.15
b	3.978 Å	O/N	4*a*	0	0	0.210	1.0/0.0
c	10.174 Å	O/N	4*a*	0	$\frac{1}{2}$	0.045	0.3/0.7
Z	4						
V	159.64 Å^3						

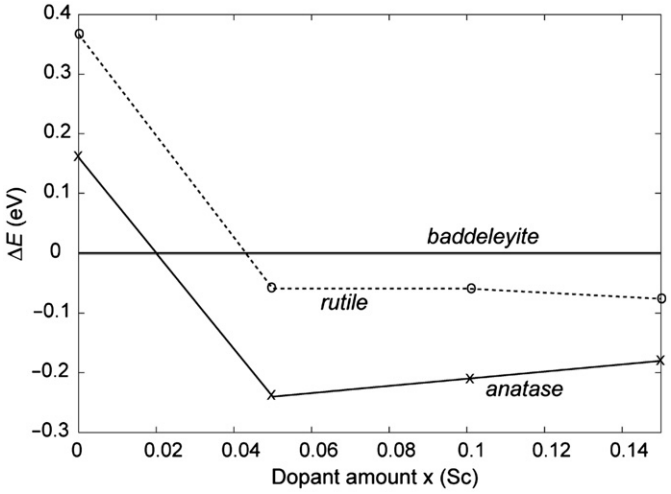

Fig. 11. Energy difference of diverse modifications as a function of scandium content.

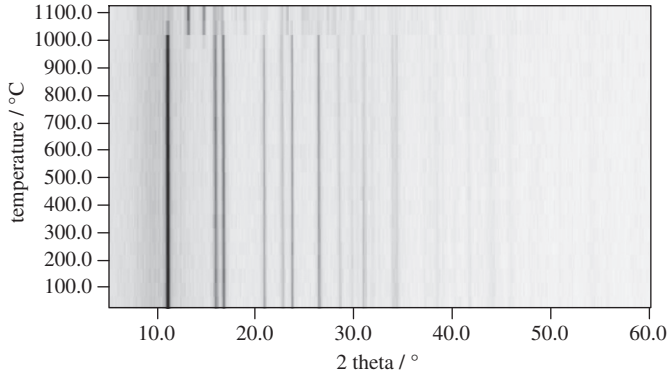

Fig. 12. High-temperature X-ray powder patterns of $Sc_{0.15}Ta_{0.85}O_{1.3}N_{0.7}$ under argon. In the temperature range between 950 and 1050 °C, a phase transformation from anatase to baddeleyite-type is observed. Intensities of the reflections correspond to the blackness of the lines.

baddeleyite-type phase is preserved after cooling, evidencing an irreversible phase transformation. Thermal expansion coefficients of $\alpha_a = 0.24 \times 10^{-5}\,K^{-1}$ and $\alpha_c = 0.90 \times 10^{-5}\,K^{-1}$ were determined from the in situ X-ray powder diffraction data (Fig. 13), yielding a volume expansion coefficient of $\gamma = 1.38 \times 10^{-5}\,K^{-1}$. Because of the different linear expansion coefficients α_a and α_c, the unit cell is

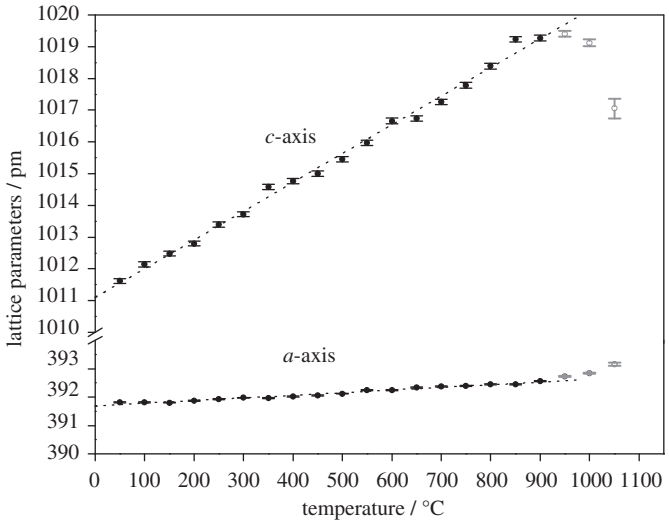

Fig. 13. Linear thermal expansion of $Sc_{0.15}Ta_{0.85}O_{1.3}N_{0.7}$ from X-ray diffraction data in the temperature range 50–1050 °C. Open symbols: transformation to baddeleyite-type.

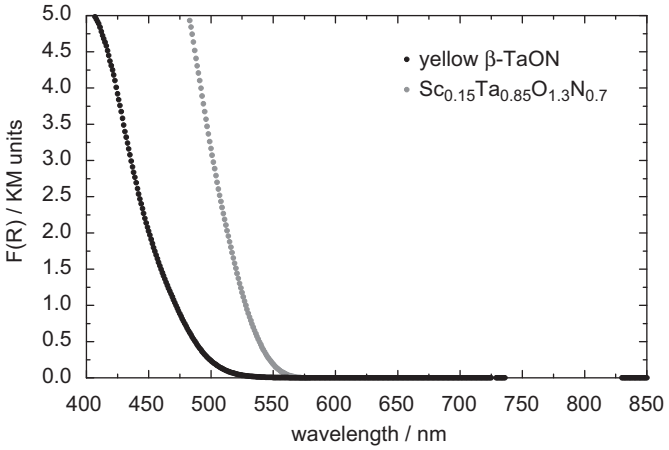

Fig. 14. UV/vis powder spectra of brick-red $Sc_{0.15}Ta_{0.85}O_{1.3}N_{0.7}$ and yellow β-TaON.

stretched in the c-direction; the c/a ratio increases from 2.58 at 25 °C to 2.60 at ~900 °C.

The wavelength of the optical absorption edge of anatase-type $Sc_{0.15}Ta_{0.85}O_{1.3}N_{0.7}$ has been determined to be 490 nm, yielding a band gap of 2.54 eV. The steep absorption edge of the mixed crystal results in the brilliant color of the compound (Fig. 14). Also in this case of anatase-type $Sc_xTa_{1-x}O_{1+2x}N_{1-2x}$ solid solutions – like in that of anosovite $Sc_xTa_{3-x}O_{2x}N_{5-2x}$, see Fig. 5 above – neither structural anion nor cation vacancies exist in the material. The absence of structural defects, therefore, appears to be a prerequisite for optically attractive materials. This supposition appears also corroborated by the optical properties of the related anatase-type phase $Mg_{0.05}Ta_{0.95}O_{1.15}N_{1.15}$, which also possesses a brilliant optical appearance [25].

4. Conclusions

In the system Sc–Ta – O – N, cubic tantalum oxide nitrides exhibiting the bixbyite-type structure were synthesized by ammonolysis of X-ray amorphous mixed oxides. These phases exist in the composition domain $Sc_xTa_{1-x}(O,N)_y$ with $0.33 \le x \le 1$

and $1.7 \leq y \leq 1.9$. The bixbyite-type can be described as a fluorite-derived structure with ordered anion vacancies and a doubling of the lattice parameters. This structure type is stable up to 900 °C. Long-range ordered anion vacancies are not desirable for good anion conductivity. Due to lattice relaxation around the vacancies, the activation energy for the jump process of the anions is strongly increased. Consequently, the phases presented here represent no promising candidates for fast anion conduction in the investigated temperature range.

Single-phase samples with anatase-type structure were also obtained, as well as phases exhibiting an anosovite-type. The anatase-type compounds are metastable and undergo a phase transformation to a baddeleyite-type phase between 950 and 1050 °C. This behavior is similar to that of anatase-type phases known from the Mg–Ta–O–N system. Both anatase- and anosovite-types materials show brilliant colors (yellow–orange–red) and are of interest as color pigments.

Acknowledgments

N/O-analysis by B. Hahn and synchrotron measurements at the HASYLAB are gratefully acknowledged. We would like to thank the computing centers at RWTH Aachen for providing large amounts of CPU time. This work was supported by the DFG within the priority program 1136.

References

[1] S. Ito, K.R. Thampi, P. Comte, P. Liska, M. Grätzel, Chem. Commun. (2005) 268.
[2] M. Hara, T. Takata, J.N. Kondo, K. Domen, Catal. Today 90 (2004) 313.
[3] R. Nakamura, T. Tanaka, Y. Nakato, J. Phys. Chem. B (2005) 8920.
[4] M. Lerch, J. Lerch, R. Hock, J. Wrba, J. Solid State Chem. 128 (1997) 282.
[5] J. Wendel, M. Lerch, W. Laqua, J. Solid State Chem. 142 (1999) 163.
[6] M.A. Taylor, M. Kilo, C. Argirusis, G. Borchardt, I. Valov, C. Korte, J. Janek, T.C. Roedel, M. Lerch, Solid State Data, Part A: Defect Diffusion Forum 479 (2005) 237–240.
[7] M. Jansen, H.P. Letschert, Nature 404 (2000) 27 980.
[8] E. Guenther, M. Jansen, Mater. Res. Bull. 36 (2001) 1399.
[9] J.H. Swisher, M.H. Read, Metall. Trans. 3 (1972) 489.
[10] M. Kerlau, O. Merdrignac-Conanec, M. Guilloux-Viry, A. Perrin, Solid State Sci. 6 (2004) 101.
[11] O. Merdrignac-Conanec, M. Kerlau, M. Guilloux-Viry, R. Marchand, N. Barsan, U. Weimar, Silic. Ind. 69 (2004) 141.
[12] M. Weishaupt, J. Strähle, Z. Anorg. Allg. Chem. 429 (1977) 261.
[13] S.J. Clarke, K.A. Hardstone, C.W. Michie, M.J. Rosseinsky, Chem. Mater. 14 (2002) 2664.
[14] C.M. Fang, E. Orhan, G.A. de Wijs, H.T. Hintzen, R.A. de Groot, R. Marchand, J.-Y. Saillard, G. de With, J. Mater. Chem. 11 (2001) 1248.
[15] E. Orhan, F. Tessier, R. Marchand, Solid State Sci. 4 (2002) 1071.
[16] D. Armytage, B.E.F. Fender, Acta Crystallogr. B30 (1974) 809.
[17] M.-W. Lumey, R. Dronskowski, Z. Anorg. Allg. Chem. 631 (2005) 887.
[18] T. Bredow, R. Dronskowski, M. Lerch, M.-W. Lumey, H. Schilling, J. Pickardt, Z. Anorg. Allg. Chem. 632 (2006) 1157.
[19] Yu.A. Buslaev, G.M. Safronov, V.I. Pachomov, M.A. Glushkova, V.P. Repko, M.M. Ershova, A.N. Zhukov, T.A. Zhdanova, Izv. Akad. Nauk SSSR Neorg. Mater. 5 (1969) 45.
[20] M.-W. Lumey, R. Dronskowski, Z. Anorg. Allg. Chem. 629 (2003) 2173.
[21] H. Schilling, A. Stork, E. Irran, H. Wolff, T. Bredow, R. Dronskowski, M. Lerch, Angew. Chem. Int. Ed. 46 (2007) 2931.
[22] G. Brauer, J.R. Weidlein, Angew. Chem. 77 (1965) 218.
[23] J. Strähle, Z. Anorg. Allg. Chem. 402 (1973) 47.
[24] W.-J. Chun, A. Ishikawa, H. Fujisawa, T. Takata, J.N. Kondo, M. Hara, M. Yasumichi, Y. Matsumoto, K. Domen, J. Phys. Chem. B 107 (2003) 1798.
[25] H. Schilling, M. Lerch, A. Börger, K.-D. Becker, H. Wolff, R. Dronskowski, T. Bredow, M. Tovar, C. Baehtz, J. Solid State Chem. 179 (2006) 2416–2425.
[26] H. Schilling, H. Wolff, R. Dronskowski, M. Lerch, Z. Naturforsch. 61b (2006) 660–664.
[27] H. Wolff, R. Dronskowski, Solid State Ionics 179 (2008) 816.
[28] M. Kilo, M.A. Taylor, C. Argirusis, G. Borchardt, M. Lerch, O. Kaitasov, B. Lesage, Phys. Chem. Chem. Phys. 6 (2004) 3645.
[29] T. Okubo, M. Kakihana, J. Alloys Compd. 256 (1997) 151.
[30] W. Kraus, G. Nolze, Bundesanstalt für Materialprüfung (BAM), Berlin, 2000.
[31] J. Rodriguez-Carvajal, Abstracts of the Satellite Meeting on Powder Diffraction of the XV Congress of the IUCr, 1990, 127.
[32] G. Kresse, J. Hafner, Phys. Rev. B 47 (1993) 558;
G. Kresse, Hafner, Phys. Rev. B 49 (1994) 14251.
[33] G. Kresse, J. Furthmüller, Comput. Mater. Sci. 6 (1996) 15;
G. Kresse, J. Furthmüller, Phys. Rev. B 55 (1996) 11169.
[34] P.E. Blöchl, Phys. Rev. B 50 (1994) 17953.
[35] J.P. Perdew, K. Burke, M. Ernzerhof, Phys. Rev. Lett. 77 (1996) 3865.
[36] E. Füglein, R. Hock, M. Lerch, Z. Anorg. Allg. Chem. 623 (1997) 304–308.
[37] S.J. Clarke, C.W. Michie, M.J. Rosseinsky, J. Solid State Chem. 146 (1999) 399.
[38] T. Bredow, M. Lerch, Z. Anorg. Allg. Chem. 630 (2004) 2262.
[39] N. Masaki, H. Tagawa, J. Nucl. Mater. 57 (1975) 187–192.
[40] R.E. Rundle, N.C. Baenzinger, A.S. Wilson, R.A. McDonald, J. Am. Chem. Soc. 70 (1948) 99–105.
[41] J.C. Phillips, Science 169 (1970) 1035.
[42] J.A. van Vechten, J.C. Phillips, Phys. Rev B2 (1971) 2160.
[43] C. K. Jorgensen, Oxidation Numbers and Oxidation States, 7, Springer Ch. 1969.
[44] F. Tessier, P. Maillard, F. Chevire, K. Domen, S. Kikkawa, J. Ceram. Soc. Jpn. 117 (2009) 1.
[45] G. Brauer, J. Weidlein, Angew. Chem. 77 (1965) 913.
[46] H. Wolff, M. Lerch, H. Schilling, C. Bähtz, R. Dronskowski, J. Solid State Chem. 181 (2008) 2684.